Effects of Aggregation on Trimeric Light-Harvesting Complex II of Green Plants: A Hole-Burning Study

J. Pieper,*,†,‡ K.-D. Irrgang,§ M. Rätsep,‡ R. Jankowiak,‡ Th. Schrötter,† J. Voigt,† G. J. Small,*,‡ and G. Renger§

Institute of Physics, Humboldt University, 10099 Berlin, Germany, Ames Laboratory, U.S. Department of Energy, and Department of Chemistry, Iowa State University, Ames, Iowa 50011, and Max-Volmer Institute, Technical University, 10623 Berlin, Germany

Received: October 5, 1998; In Final Form: December 10, 1998

Low-temperature absorption, fluorescence, and persistent hole-burned spectra are reported for aggregates of the trimeric light-harvesting antenna complex of photosystem II (LHC II) . The lowest energy Q_y-state was found to lie at 681.5 nm on the basis of hole spectra, which corresponds to a 2 nm red shift relative to the isolated LHC II trimer (Pieper et al. *J. Phys. Chem. B* **1999**, 2412, accompanying paper). The electron−phonon coupling of the 681.5 nm state is characterized by $S \sim 0.8$ and coupling to phonons with a mean frequency of ~ 20 cm^{-1} which is very similar to that of the isolated trimer. This coupling is consistent with the 4.2 K Stokes shift of the fluorescence originating from the 681.5 nm state. An adjacent state at 680.0 nm is assigned. On the basis of the results of Pieper et al. for the isolated trimer, a state at $\sim$ 678.5 nm is inferred. These three lowest energy Q_y-states are associated with the lowest energy chlorophyll *a* state of the subunit of the isolated LHC II trimer. Their degeneracy is removed because of structural heterogeneity. The hole-burning results indicate that, aside from a quite uniform and small red shifting, aggregation has little effect on the excitonic level structure and intrinsic dynamics of the isolated trimer. Taken together, the results presented here and in Pieper et al. lead to a model that qualitatively accounts for the strong temperature dependence of aggregation-induced fluorescence quenching between 4.2 and 80 K (Ruban et al. *Biochim. Biophys. Acta* **1992**, *1102*, 30).

1. Introduction

The adaptation of photosynthetic organisms to different illumination conditions predominantly takes place via regulation of excitation energy transfer (EET) processes within pigment−protein complexes which act as the antenna. In general, these antenna systems exert a dual role: (i) at low light intensities excited singlet states, generated by the few quanta absorbed, are funneled with high efficiency to the primary electron donor of the reaction center (for reviews, see Renger[1] and van Grondelle et al.[2]) and (ii) under light stress superfluous excitation is dissipated by radiationless decay processes to prevent or diminish harmful reactions (for a review, see Horton et al.[3]).

The most abundant light harvesting complex is the integral membrane bound Chl *a*/*b* containing LHC II of green plants which binds about 50% of the total chlorophyll content of the thylakoids. Together with minor integral pigment protein complexes, LHC II forms the peripheral and proximal antenna of photosystem II and is linked to the reaction center by the Chl *a* binding proteins CP 47 and CP 43 which are referred to as core antenna (for reviews, see Jansson,[4] Zuchelli et al.,[5] Paulsen,[6] Green and Dunford,[7] and Bassi et al.[8]).

As discussed in the accompanying paper[9] (referred to hereafter as I), considerable progress has been made toward understanding the ground-state structure, $Q_y(S_1)$-electronic states and EET processes of isolated LHC II trimers which are believed to be the predominant in vivo form. Of particular relevance to this paper is that in I spectral hole burning was used to identify the three lowest Q_y-states of the trimer which lie at 679.8, 678.4, and 677.1 nm at liquid helium temperatures. These states were assigned to the lowest energy (predominantly Chl *a*) state of each of the three subunits of the trimer with the $\sim$30 cm^{-1} splitting between them due to structural heterogeneity. Currently, each subunit is believed to contain seven Chl *a* and five Chl *b* molecules.[10]

The present paper is the result of our interest in the recent finding that reversible aggregation of LHC II trimers in vitro leads to formation of singlet quencher states as reflected by fluorescence lifetime[11,12] and quantum yield[13] data as well as a red shifting of the fluorescence origin band region.[14] It was inferred that aggregation in vivo serves as a protective mechanism for dissipation of excess excitation energy via radiationless decay.[8] The static fluorescence spectrum of isolated LHC II trimers at 77 K is dominated by an origin band at 680 nm which decay-associated fluorescence spectra (DAS) showed corresponds to an excited state with a lifetime of 5 ns.[12] Lowering the temperature to 4.2 K has little effect on this lifetime or position of the origin which at 4.2 K is 680.3 nm (see I). Aggregation results in 77 K fluorescence spectra that show additional structure to the red of the highest energy band at 683 nm. For samples prepared by the Triton X-100 procedure,[15] there is a comparably intense and broader band at 702 nm.[11,12] For samples prepared by the β-dodecylmaltoside (DM) procedure,[16] the 702 nm band is absent although there is a

† Institute of Physics.
‡ Ames Laboratory.
§ Max-Volmer Institute.
* Author to whom correspondence should be addressed.

10.1021/jp983958d CCC: $18.00
Published on Web 02/17/1999

distinct shoulder at 695 nm.[12] At liquid helium temperatures the 683 nm band remains intact but the 702 and 695 nm bands of the Triton X-100 and DM samples vanish.[12] The 10 K static fluorescence spectra of the two types of aggregate sample are very similar. Recently, DAS results have been obtained for both aggregate sample types at 10 and 80 K.[12] Both exhibit at least three red-emitting states ($\lambda \geq 683$ nm) with nanosecond lifetimes and two states with ~150 and 500 ps lifetimes which, at 10 K, emit near 680 and 682 nm. At both temperatures the peak amplitudes of the two quenched states dominate those of the red-emitting states, significantly more so at 80 K. Some significant differences between the DAS spectra for the two sample types exist. On the basis of these spectra, the static fluorescence spectra and the temperature dependence of the overall fluorescence yield it could be concluded that the above red-emitting states are not the quenching states.[11,12] It was concluded in[12] that a distribution of aggregate sizes is not responsible for the multicomponent emission. The nature of the quenching states and the biological significance of the red-emitting states remain as open questions. In general, the formation of aggregates can be expected to give rise to structural changes that modify pigment−pigment and/or pigment−protein interactions, thereby resulting in quenching states. Evidence for structural changes has been provided by resonance Raman[17] and linear/circular dichroism studies at 77 K.[18]

As discussed in detail in ref 12, understanding the aforementioned effects of aggregation is a complex problem that requires additional experiments for solution. In this paper we report the results of hole-burning and static fluorescence experiments which, together with the results of I, allow us to assess the extent to which aggregation affects the electronic structure and dynamics of the isolated LHC II trimer and to identify absorption due to the red-emitting states. The results for the aggregate samples together with those for the isolated trimer lead to a model that qualitatively explains the significant decrease ($\times 7$) in fluorescence quantum yield as the temperature is increased from 4 to 77 K.[14] Experiments were confined to aggregate samples obtained using the well-defined and biochemically thoroughly characterized β-dodecyl maltoside preparation of solubilized LHC II trimers developed by Irrgang et al.[16] The biochemical properties are described in Schödel et al.[19]

2. Experimental Section

LHC II preparations were isolated by solubilization of salt washed PS II membrane fragments of spinach in the presence of β-dodecyl maltoside (DM) and separation by sucrose density gradient centrifugation as described in detail previously.[16] Aggregated complexes were obtained by dialysing the solubilized samples for 48 h at 4 °C in the dark against a detergent-free buffer solution containing 30 mM MES−NaOH, pH 6.5, 15 mM NaCl, 5 mM $MgCl_2$. Pigment concentration (vide infra) and a Chl a/b ratio of 1.35 ± 0.05 were determined using the method of Porra et al.[20] The polypeptide composition of isolated LHC II was checked by SDS/urea/PAGE using the method described in ref 16 in combination with silver staining and immunoblotting experiments as described in detail in ref 12. Besides the $LHCb_{1-3}$ gene products of the major light-harvesting complex, the β-DM solubilized LHC II also contains all but one of the minor Chl *a/b* binding proteins (CP 14/15, CP 22, CP 24, and CP 26) known to be associated with the antenna system of photosystem II.[12] It is CP 29 that is missing. According to densitometrical scanning of silver-stained polyacrylamide gels, 87.4% of the apoproteins could be ascribed to $LHCb_{1-3}$ proteins and 12.6% to the minor pigment−protein complexes, mainly CP 24 and CP 26. For low-temperature experiments aggregated LHC II was diluted with a glass forming buffer solution containing 30 mM MES−NaOH, pH 6.5, 15 mM NaCl, 5 mM $MgCl_2$, and 70% w/v glycerol. The total chlorophyll concentration of the sample was 0.007 and 0.200 mg Chl/ mL for hole-burning and fluorescence measurements, respectively.

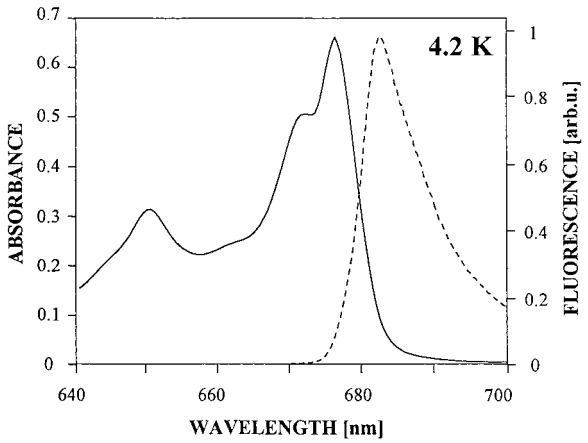

Figure 1. Absorption (full line) and fluorescence spectrum (dashed line) of aggregated LHC II complexes at 4.2 K.

The hole-burning apparatus used is described in the accompanying paper (I)[9] and references therein. Zero-phonon holewidths reported were measured at a resolution of 0.3 cm^{-1} (burn laser line width = 0.05 cm^{-1}). The sample temperature was 4.2 K. Burn fluences and wavelengths and read resolutions are given in the figure captions.

Fluorescence measurements employed a N_2-laser pumped dye-laser (Laser Science, Inc., VSL-Dye) of about 3 ns duration and a repetition rate of 20 Hz for excitation. Samples were excited at 430 nm. The applied pulse energy was approximately 10^{13} photons per cm^2 per pulse. The fluorescence signal was measured employing a double monochromator (Carl Zeiss Jena, GDM 1000, spectral resolution of 0.5 nm) and an avalanche diode (type 712-A4). The samples were cooled in an Oxford helium flow cryostat (type Optistat). The optical density of the sample at 4.2 K was 0.02 at 676 nm in a 0.01 mm cuvette. There was no detectable influence of reabsorption under these conditions.

3. Results

The 4.2 K absorption spectrum of aggregated LHC II trimers shown in Figure 1 exhibits four main bands at 676.3, 671.9, 662.0, and 650.5 nm which are red-shifted by 1 nm relative to those of the isolated trimer; see I. Other than this slight uniform shifting, the Q_y-spectra of the aggregate and isolated trimer are essentially identical. The 4.2 K fluorescence origin band of the aggregate shown in Figure 1 exhibits a maximum at 682.6 nm which is red shifted by 2.3 nm relative to that of the isolated trimer, see I. In addition, the origin band of the aggregate is broader and exhibits considerably more tailing to the red, consistent with the existence of red emitters. The 77 K fluorescence spectra of the aggregate and isolated trimer are shown in Figure 2. The fluorescence origin band of the aggregate at 681.7 nm is red shifted by 2.3 nm relative to that of the isolated trimer. In addition to this shift, the red tailing of the aggregate fluorescence and the distinct shoulder near 695 nm mentioned in the Introduction are apparent. The red shifting of the aggregate is also seen in the vibronic region near 740 nm. The fluorescence results of Figures 1 and 2 are consistent with

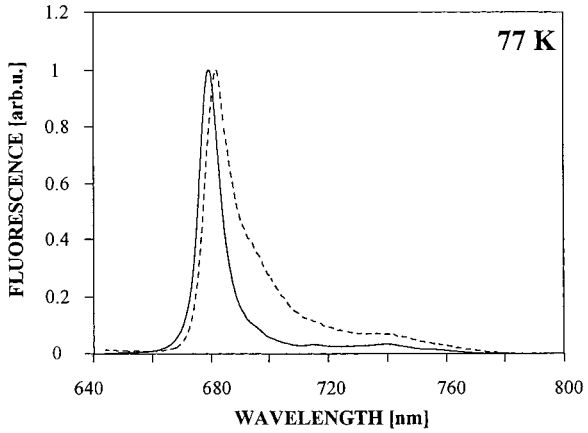

Figure 2. Normalized fluorescence spectra of solubilized (full line) and aggregated (dashed line) LHC II complexes at 77 K.

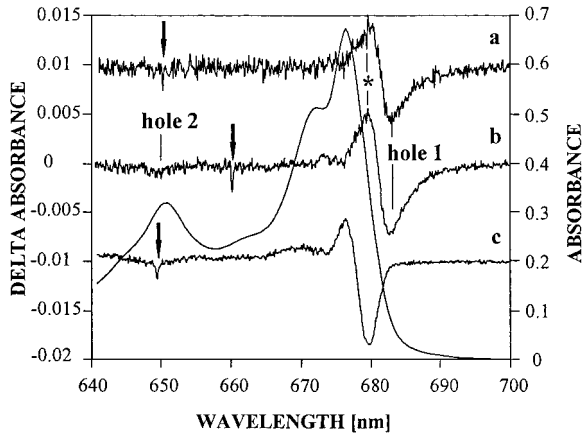

Figure 3. Typical hole burned spectra of aggregated (spectra a and b) and solubilized LHC II trimers (spectrum c) obtained with a burn laser intensity of 100 mW/cm^2 and a read resolution of 4.0 cm^{-1}. The burn wavelengths and burn times were (spectrum a) 649 nm and 10 min, (spectrum b) 660 nm and 30 min, (spectrum c) 648.6 nm and 10 min, respectively. The arrows indicate the burn wavelengths. Hole-burned spectra are separated by a ΔA of 0.01. Spectra a and c are enlarged and compressed by a factor of 2, respectively. The 4.2 K absorption spectrum of aggregated LHC II is given for comparison.

those of Vasiliev et al.[12] It is important to note that the intensity of the static fluorescence at 77 K was observed to be about an order of magnitude weaker than at 4.2 K, consistent with the results of Ruban et al.[13]

Hole burning of LHC II aggregates was performed with burn wavelengths (λ_B) between 640 and 688 nm for different burn fluences. As observed in I for solubilized LHC II trimers, the burn efficiency markedly decreases for λ_B shorter than ~676 nm. Traces a and b of Figure 3 show hole-burned spectra of aggregated LHC II which are quite typical for the burn fluences used and λ_B < 676 nm (the arrows in Figure 3 indicate the burn wavelengths). The most obvious features of these spectra are (a) a zero-phonon hole (ZPH) coincident with the burn wavelength, (b) a broad hole (hole 1) in the vicinity of 682.5 nm having a width of about 80 cm^{-1}, and (c) a broad and shallow hole (hole 2) at about 650 nm that appears only at sufficiently high burn fluence (see trace b and I for similar behavior of the LHC II trimer). The feature labeled by the asterisk in Figure 3 is the antihole of hole 1. For all burn wavelengths employed, the most intense feature of the hole-burned spectrum is hole 1 located in the low-energy wing of the 676.3 nm absorption band. As is the case for the LHC II trimer (see I), hole 1 for the aggregate undergoes a slight blue

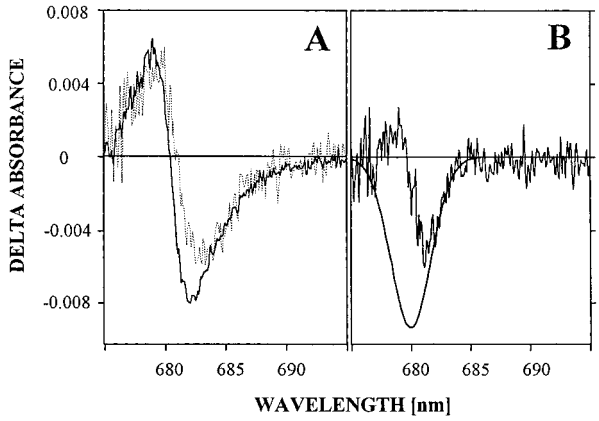

Figure 4. Frame A: 4.2 K hole-burned spectra of aggregated LHC II obtained with λ_B = 660. nm and a burn intensity of 100 mW/cm^2. The darker and lighter spectra were obtained with burn times of 30 and 1 mm, respectively. Frame B: Noisy spectrum is the difference between the two spectra of part A and is peaked at 681.5 nm. The Gaussian profile of the ZPH-action spectrum is shown for comparison.

shifting with increasing burn fluence. For example, with a burn intensity of 100 mW/cm^2 and burn times of 1 and 30 min, hole 1 is centered at 683.0 and 682.0 nm, respectively, see frame A of Figure 4. For the 30 min burn time, hole 1 is close to saturated. The blue shifting was interpreted in I as a manifestation of hole 1 being contributed to by three states associated with the lowest energy state of the subunit of the trimer which are rendered energetically inequivalent due to structural disorder. On the basis of the results of I, one might conclude that hole 1 of the aggregate also represents these three states of the trimer which are populated from higher energy states by efficient energy transfer. However, more careful inspection reveals that this is not entirely correct. A hole-burned spectrum from I for the isolated LHC II trimer is shown as spectrum c in Figure 3 with hole 1 located at 680 nm, about 3 nm to the blue of hole 1 of aggregated LHC II (spectra a and b). For comparable burn fluences, hole 1 of the isolated trimer and aggregate is located at 679.4 and 682.5 nm, respectively. This shift is about 3 times larger than the shift of the principal absorption bands. At the same time, the width of hole 1 increases from 55 cm^{-1} to about 80 cm^{-1}. It should be noted, however, that a precise determination of the position and width based on the spectra shown in Figure 3 is not possible because of interference between the hole and its antihole (see I). The observed broadening of hole 1 upon aggregation is most likely mainly connected with the tailing of its low energy wing. (The antihole of hole 1 for the aggregate tails more slowly to higher energy of its maximum than that of the isolated trimer, especially for low burn fluences, spectrum a.) This tailing is ascribed in the following section to the aggregation-induced, red-emitting states lying at wavelengths $\gtrsim$683 nm.

Burn efficiencies and widths of ZPH burned at wavelengths 640 nm < λ_B < 670 nm closely resemble those observed for solubilized LHC II presented in I. The broad Chl *b* hole (hole 2) for the aggregate lies at 650.2 ± 0.3 nm. This represents a red shift of about 2 nm compared to its position at 648.3 ± 0.3 nm in the isolated trimer while its width of ~ 125 cm^{-1} is the same as that of the isolated trimer.

As in I, constant fluence hole-burning (ZPH action) spectroscopy was employed in order to further investigate the spectral position and inhomogeneous width of the lowest state(s). The ZPH action spectrum obtained for a burn fluence of 6 J/cm^2 and a read resolution of 0.3 cm^{-1} is shown in Figure 5. It is centered at 680 nm and can be fitted by a Gaussian

TABLE 1: Zero-Phonon Holewidths and Total Dephasing Times

	4.2 K/λ_B (nm)						
	677.0	678.0	679.0	680.0	681.0	682.0	683.0
$\Delta A/A$[a]	0.01	0.03	0.06	0.10	0.12	0.15	0.11
Γ_{hole} (cm^{-1})[b]	2.0 ± 0.4	1.8 ± 0.4	1.1 ± 0.3	0.8 ± 0.2	0.7 ± 0.2	0.6 ± 0.1	0.6 ± 0.1
Γ_{hom} (cm^{-1})[c]	0.9 ± 0.2	0.7 ± 0.2	0.5 ± 0.2	0.3 ± 0.1	0.2 ± 0.1	0.15	0.15
T_2 (ps)[d]	12 ± 3	15 ± 5	20 ± 10	40 ± 10	~100	*e*	*e*

[a] Fractional absorbance change of hole. [b] Measured holewidth, uncorrected for read resolution of 0.3 cm^{-1}. [c] Homogeneous width of zero-phonon line, corrected for read resolution. [d] Total optical dephasing time. [e] Resolution inadequate for determination.

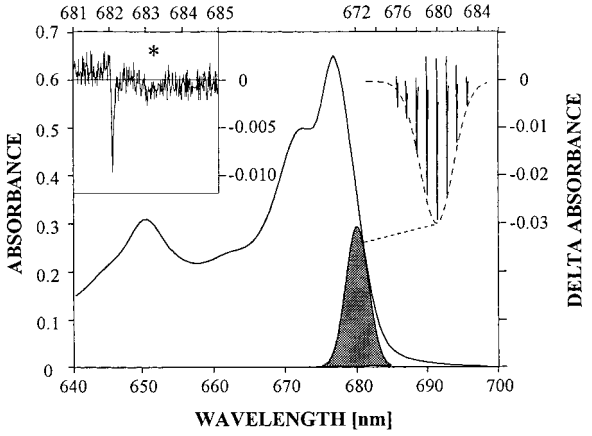

Figure 5. The 4.2 K absorption spectrum and ZPH-action spectrum (upper right corner) of aggregated LHC II trimers. The profile of the action spectrum centered at 680.0 nm is Gaussian with a width of 85 ± 10 cm^{-1}. Its position within the absorption spectrum is indicated by the hatched profile to the right of the maximum of the 677 nm absorption band. The action spectrum was generated with a constant burn fluence of 6 J/cm^2 and read resolution of 0.3 cm^{-1}. The left inset shows a hole burned spectrum obtained with $\lambda_B = 682.0$ nm, a burn intensity and time of 40 mW/cm^2 and 2 min, and a read resolution of 0.5 cm^{-1}. The pseudo-PSBH is indicated by the asterisk.

envelope with a width of 85 ± 10 cm^{-1}. This means, surprisingly, that the efficiency for selective burning of ZPH decreases markedly for burn wavelengths $\lambda_B \geq 684$ nm even though tailing of hole 1 is observed in this very spectral region when burning nonselectively at shorter wavelengths, vide supra. Implications of the absence of ZPH for $\lambda_B \geq 684$ nm are considered in the following section. The widths of the ZPH (uncorrected for read resolution) decrease from 2.0 cm^{-1} (677 nm) to 0.6 cm^{-1} (681−683 nm) at the low-energy wing of the action spectrum, Table 1. The broader ZPH observed at the high-energy wing of the action spectrum most probably stem from downward energy transfer from states associated with the main 676.3 nm absorption band and energetically inequivalent sublevels of the lowest state associated with the subunit of the trimer complex as concluded in I for the isolated trimer, vide infra.

A comparison of the above aggregate results with the results in I for the solubilized trimer shows that, upon aggregation, the lowest energy state(s) of the isolated trimer are basically red shifted by about 2 nm. At the same time, the width of the inhomogeneous distribution function and the homogeneous widths of the ZPH associated with the action spectrum are hardly affected. This also applies to the observed narrowing of the ZPH when the burn wavelength is tuned from the blue to the red sides of the action spectrum. Therefore, we conclude that the low energy level structure of isolated LHC II remains almost intact upon aggregation except for the slight red shifting. A more detailed inspection of the low energy absorption near 680 nm of solubilized LHC II given in I revealed that it is contributed to by three states, with the lowest one lying ~1.5 nm to the red of the maximum of the action spectrum. In view of the similarities between the aggregate and the isolated trimer one can infer, by analogy, that the lowest energy state/sublevel of aggregated LHC II represented by the action spectrum is located at 681.5 ± 0.4 nm. In the following section this assignment is shown to be consistent with the fluorescence Stokes shift and other results.

The data discussed above indicate that hole 1 does not solely originate from a burn process within the above assigned three lowest energy states. Neither the position of the action spectrum at 680.0 ± 0.2 nm nor that of the lowest state at 681.5 ± 0.4 nm is in agreement with the value of 682.5 nm for the broad hole 1. Therefore, it has to be concluded that aggregated LHC II is characterized by additional weak absorption at $\lambda \geq 683$ nm that does not contribute to the action spectrum and may reflect the long-wavelength spectral components that were assigned in steady-state fluorescence and fluorescence decay experiments, cf. Introduction. Further discussion is given in the following section.

The left inset of Figure 5 shows a shallow ZPH (fractional absorbance change of 0.1) burned at 682.0 nm, i.e., at the low-energy side of the ZPH action spectrum. It is accompanied by a shallow and broad feature located by the asterisk which is displaced from the ZPH by about 20 cm^{-1}. The ratio of the integrated intensities of this pseudo-phonon sideband hole (pseudo-PSBH) and the ZPH was used to obtain an upper limit for the Huang−Rhys factor S of 0.8. Thus, the weak phonon coupling ($S = 0.8$) to phonons with a mean frequency of 18 cm^{-1} observed for the isolated LHC II trimer (see I) remains unaffected by aggregation. The real PSBH was not discernible for aggregated LHC II because it is interfered with by the antihole of the pseudo-PSBH and ZPH.

4. Discussion

Effects of Aggregation on the Exciton Level Structure of the LHC II Trimer. As pointed out in the Introduction, aggregation leads to pronounced fluorescence quenching of the LHC II trimer that depends strongly on temperature in the ~4−80 K range. However, comparison of the 4.2 K absorption spectrum of the aggregate (Figure 1) with that of the isolated trimer given in I shows that the major effect of aggregation is to only uniformly shift the Q_y-absorption spectrum to the red by ~1 nm. By itself, this small shift indicates that strong excitonic interactions between neighboring trimers of the aggregate do not exist and, furthermore, that aggregation does not alter Chl−protein interactions of the trimer to a significant extent. The slight red shifting is most likely mainly a manifestation of stabilization of the Q_y-states of a given trimer by dispersion and van der Waals interactions between its Chl molecules and the protein of surrounding trimers and/or aggregation-induced structural changes[17,18] rather than excitonic coupling between Chl molecules belonging to different trimers. To a first approximation, the coupling between Chl molecules belonging to different trimers should be as weak as those

between Chl molecules belonging to different subunits of the trimer, ≤ 5 cm^{-1} according to ref 21. The effects of such weak coupling would be significantly depressed by virtue of structural heterogeneity which leads to energetic inequivalence between symmetry equivalent Chl molecules. Furthermore, excitonic coupling would not be expected to give rise to a more or less uniform red shifting. Strong support for aggregation having little effect on the Q_y-electronic structure of the isolated trimer is provided by the hole-burned spectra. First, comparison of the hole-burned spectra for the aggregate obtained with $\lambda_B \leq 676$ nm, Figure 3, with those of the isolated trimer presented in I reveals that their main features are very similar and, furthermore, that their nonphotochemical hole burning efficiencies are comparable. The latter comparison is based on the burn fluences used and the resulting absorbance changes associated with the holes. Second, the ZPH action spectrum of the aggregate shown in Figure 5 exhibits an inhomogeneous width of 85 ± 10 cm^{-1} which, within experimental uncertainty, is the same as that for the isolated trimer; see I. The action spectra are well described by a Gaussian profile with the maximum for the aggregate located at 680.0 nm, a wavelength that is shifted by 2 nm to the red relative to the value for the isolated trimer. Third, the dependence of the width of the ZPH associated with the action spectrum on λ_B given in Table 1 for the aggregate is very similar to that of the isolated trimer (see Table 2 of I). That is, the widths of the ZPH decrease from 2.0 cm^{-1} on the high energy side of the action profiles to $\sim$ 0.6 cm^{-1} on the low energy side (read resolution of 0.3 cm^{-1}). The implications of these widths for dynamics are considered later. Fourth, the results in frame A of Figure 4 for hole 1 (see Figure 3) show that the maximum of hole 1 shifts to the blue by up to $\sim$1 nm as the burn fluence is increased. Precisely the same behavior is observed for the isolated trimer; see I. In I, the blue-shifting effect was linked to the existence of three states at 677.1, 678.4, and 679.8 nm which are the lowest energy states of the isolated trimer. Because the 679.8 nm state at 4.2 K has a $\sim$5 ns lifetime it undergoes nonphotochemical hole burning first since the lifetimes of the two higher energy states due to downward energy transfer are tens of picoseconds. These two states, however, can undergo hole burning following completion of hole burning in the 679.8 nm state. The difference between the two spectra of frame A of Figure 4 is shown in frame B along with the Gaussian profile of the ZPH action spectrum with a width of 85 cm^{-1}. The maximum of the difference spectrum is at 681.5 nm which, based on the arguments given in I, we assign as the wavelength of the lowest energy state of the trimer in the aggregate. The inhomogeneous width of the difference profile is 70 cm^{-1}. As in I, it was found that the ZPH action profile can be fitted by three equiintense Gaussians of equal intensity and a width of 70 cm^{-1}, but located at 681.5, 680.0, and $\sim$678.5 nm.

Support for the assignment of the lowest energy state of the trimer in the aggregate at 681.5 nm is provided by the 4.2 K fluorescence origin band, Figure 1, which lies at 682.6 nm. On the basis of the inset spectrum of Figure 5 (and others not shown) which shows a ZPH and pseudo-PSBH, a value of $S = 0.8$ and $\omega_m = 20$ cm^{-1} for the linear electron−phonon coupling was determined. ω_m is the mean frequency of the phonons that couple to the optical transition. Because the difference profile of the 681.5 nm state given in Figure 4 represents a zero-phonon transition profile, the nonline narrowed fluorescence origin band should be displaced to lower energy of it by $S\omega_m = 16$ cm^{-1}. This leads to a wavelength of 682.3 nm for the origin band which is in satisfactory agreement with the experimental value of 682.6 nm.

We turn next to the question of the absorption intensity of the three lowest energy states which are mainly responsible for the ZPH action spectrum shown in Figure 5. Its hatched Gaussian profile is shown below the low energy side of the 676 nm absorption band and is positioned at 680.0 nm, the observed maximum of the action spectrum. The procedure given in I was used to adjust its intensity. It involves, in part, taking into account the absorbance changes of saturated ZPH on the low energy side of the action spectrum as well as the value of 0.8 for the Huang−Rhys factor *S*. It was found that the absorption due to the three lowest energy states constitutes 8% of the total integrated intensity of the Q_y-absorption spectrum, a value that is similar to the value of 9% obtained for the isolated trimer. This is further evidence for aggregation having only a weak effect on the exciton level structure of the isolated trimer.

However, from Figure 5 it is apparent that there is residual absorption at wavelengths $>\sim$683 nm. This absorption has a maximum at $\sim$684 nm, carries a width of 240 cm^{-1}, and contributes 1.4% of the total intensity of the Q_y-absorption spectrum. The residual absorption is much weaker for the isolated trimer (see I). Therefore, we associate it with the red-emitting states of the aggregate discussed in the Introduction. This assignment is viewed as reasonable since the red tailing of the fluorescence band at 4.2 K shown in Figure 1 is far more pronounced than that of the isolated trimer (see Figure 8 of I). Simulation of the nonline narrowed fluorescence origin band of the isolated trimer using the theory of ref 22 showed that it can be accounted for using the values for linear electron−phonon coupling parameters and inhomogeneous broadening given in I (to be published). This is not the case for the aggregate, which one would expect if the red emitting states are populated by energy transfer within the aggregate of LHC II trimers and minor protein complexes. We defer discussion of the red-emitting states until the following subsection.

Aggregation-Induced Fluorescence Quenching. An important step toward understanding the quenching of LHC II trimer fluorescence in aggregates would be to understand why the quenching at 80 K is 7 times more efficient than at liquid helium temperatures, while the dependence on temperature above 80 K is weak.[13] We believe that the hole burning results provide a plausible explanation. These results show that, aside from a slight red shifting, the Q_y-state (exciton level) structure of the LHC II trimer in the aggregate remains intact. The three lowest energy states of the trimer in the aggregate at 4.2 K lie at 681.5, 680.5, and $\sim$678.5 nm. The splitting between these states is about 30 cm^{-1}, which is large relative to kT at 4.2 K but comparable to kT at 80 K (55 cm^{-1}). In I, the three lowest energy states of the isolated trimer were assigned to the lowest energy state (predominantly Chl *a* in character) of the subunit of the trimer with the $\sim$30 cm^{-1} splittings being due to structural heterogeneity. It was concluded that these states are quite highly localized on a single Chl *a* molecule of the subunit since the excitonic coupling energies between Chl molecules belonging to different subunits are small (≤ 5 cm^{-1}) relative to the inhomogeneous broadening ($\sim$80 cm^{-1}).

Both the hole burning data of I and the pump−probe results of Savikhin et al.[23] for the isolated trimer indicate that at liquid helium temperatures downward relaxation of the two higher energy states occurs in about 10 ps. This is also the case for the aggregate, vide infra. Therefore, one expects that excitation should be localized in the 681.5 nm state on the same time scale and that this localization precedes intertrimer transfer, vide infra.

We emphasize that it is the migrating exciton created by this state whose fluorescence is expected to be quenched. The situation is different at 80 K where the two higher energy states are significantly thermally populated. A model in which the aggregate is viewed as a two-dimensional, close-packed array of trimers, predicts that the number of effective pathways at 80 K for energy transfer from a given trimer to neighboring trimers is about 9 times greater than that at 4.2 K. In arriving at this factor it was taken into account that at 4.2 K an excited subunit of a trimer corresponding to the 681.5 nm state can only transfer to a nearest neighbor subunit of another trimer if the lowest excited state of that subunit is the 681.5 nm state. Thus, under the reasonable assumption that the first step of the process that leads to fluorescence quenching is energy transfer between trimers, the above model accounts for the strong temperature dependence between 4 and 80 K and, also, the weak dependence on temperature above 80 K.[13] Energy transfer within the aggregate leads mainly to population of nonradiative trap states, not the red-emitting states that contribute to the low-energy tailing of the fluorescence origin band.[11,12]

The zero-phonon holewidths given in Table 1 for seven burn wavelengths between 677.0 and 683.0 nm, which span the range from the high to low energy sides of the ZPH action profile, are identical to those given in I for the isolated trimer when the ~2 nm red shifting of the ZPH action spectrum of the aggregate is taken into account. Γ_{hom} in Table 1 is the homogeneous width of the zero-phonon line calculated from the width of the hole (Γ_{hole}) using $\Gamma_{hom} = (\Gamma_{hole} - 0.3)/2$, where the 0.3 corrects for the instrumental read resolution of 0.3 cm^{-1} (see I where it is shown, using 20 MHz read resolution data, that this formula is quite accurate). The bottom line of Table 1 gives the total dephasing times in ps calculated according to $T_2 = (\pi\Gamma_{hom}c)^{-1}$, where $c = 3 \times 10^{10}$ cms^{-1}. When the dephasing is due to depopulation by energy transfer, $T_2 = 2T_1$ where T_1 is the lifetime. As in I, we assign the T_2-values for the four shortest burn wavelengths to downward energy transfer associated with the 680.5 and ~ 678.5 nm states. For $\lambda_B = 677.0$ and 678.0 nm, states associated with the 676 nm absorption band also probably contribute to the holewidth. The energy transfer times range from ~6 ps at 677 nm to 20 ps at 680.0 nm. Of particular interest to this paper are the holewidths of 0.6 ± 0.1 cm^{-1} for $\lambda_B = 682.0$ and 683.0 nm which, according to our analysis, should lie mainly in the inhomogeneously broadened absorption profile of the lowest energy state of the trimer in the aggregate. Since the read resolution is only 0.3 cm^{-1}, there is considerable uncertainty in the values of 0.15 cm^{-1} for Γ_{hom}. In addition, it was shown in I (using 20 MHz resolution data) that pure dephasing due to coupling with the glassy two-level systems of the system dominate the optical dynamics of the lowest energy state of the isolated trimer at 4.2 K. This is probably also the case for the aggregate. In view of this, it is reasonable to assert that the contribution to Γ_{hom} from energy transfer between trimers can be no greater than ~0.1 cm^{-1}, which means that the lifetime of the lowest state of a given trimer at 681.5 nm due to energy transfer can be no shorter than ~50 ps. As discussed in the Introduction, time-resolved decay associated spectra (DAS) obtained at 10 K revealed a ~140 ps component near 680 nm. A 540 ps kinetic component near 682 nm with amplitude comparable to that of the 140 ps component was also observed. The quenching process involves three steps: escape of the excitation from the initially excited trimer, migration of the excitation to the quencher species, and capture by the quenching state. The ZPH widths discussed above speak only to the kinetics of the first step. The DAS define the lifetimes and wavelengths of the emitting species. The time-resolved fluorescence measurements failed to identify the quenching states although it was convincingly shown that they are not the observed red-emitting states with nanosecond lifetimes.[11,12] It is also clear from those works that the fluorescence being quenched is that of the main origin band which lies at 681.5 nm at liquid helium temperatures. Specifically, it would be the fluorescence of the migrating trimer exciton that is quenched. The associated 140 and 540 ps components might represent two distinct migratory pathways to the quenching site(s) (assuming that capture at such sites is fast relative to migration). Alternatively, they might simply reflect the fact that the migration kinetics are quite highly dispersive due to disorder in the aggregate. In this regard, detailed studies of the rise times of the wavelength-dependent fluorescence decay components might prove useful. They might also shed light on the exciton migration times. On the basis of hole-burning data it appears that, following excitation of a trimer, the time required to reach a quenching site should be longer than ~50 ps at low temperatures.

Our results say nothing about the nature of the highly nonradiative quenching states. Thus, this question remains open.[12] It was suggested in that reference that the quenching may be due to states (Chl *a* species) resulting from interactions between the minor protein complexes, such as CP 24 and CP 26, and LHC II trimers in the aggregate. Studies in which the number and concentration of the minor complexes are varied would test this suggestion. The hole-burning results do suggest that interactions between neighboring LHC II trimers in the aggregate are not primarily responsible for the formation of the quenching species. This follows since our results establish that, aside from slight red shifting, the Q_y-level structure of the isolated trimer are not significantly perturbed by aggregation. That the quenching states are highly nonradiative suggests that the species involved might be a Chl *a* dimer with a configuration that is conducive to radiationless decay. One possible mechanism for such decay is charge separation.

To conclude this section we consider the red-emitting, nanosecond lifetime states at wavelengths ≥ 684 nm which were identified in absorption by nonselective hole burning at shorter wavelengths. It was the tailing to the red of hole 1 (spectra a and b of Figure 3) that was correlated with the residual red absorption which analysis of the results shown in Figure 5 indicated is located at ~684 nm with a broad width of 240 cm^{-1}. Although the states associated with the residual absorption undergo hole burning following transfer of excitation energy to them, we were unable to burn sharp ZPH upon selective excitation in the residual absorption region. One possible explanation for the absence of ZPH is that they are Franck−Condon forbidden. This forbiddeness would be expected for states with significant charge-transfer character since such character leads to strong electron−phonon coupling.[24] If this were to be the case, then it would lend support to the idea that the yet to be characterized quenching states carry significant charge-transfer character because of a special geometry associated with interacting Chl *a* molecules.

5. Concluding Remarks

Comparison of the hole spectra for the isolated LHC II trimer given in I with those of the aggregate leads to the conclusion that aggregation has little effect on the Q_y-electronic structure and intrinsic excitation energy transfer dynamics of the isolated trimer. The main effect appears to be a slight, more or less uniform red-shifting of the Q_y-states by ~2 nm. The three lowest

energy states of the isolated trimer are associated with the lowest energy (mainly Chl *a*) state of the subunit of the trimer (see I). The splittings between these states of $\sim$30 cm^{-1} is most likely due to structural heterogeneity. This level structure is preserved in the aggregate, the only difference being that in the aggregate the three lowest energy states are slightly red-shifted to 681.5, 680.0, and $\sim$ 678.5 nm. This finding led to a simple model that explains why aggregation-induced quenching of the trimer fluorescence is about a factor of 10 times more efficient at 80 K than at 4 K. This model, which pictures the aggregate as a two-dimensional array of "close-packed" trimers, predicts that the number of pathways for transfer of energy from the initially excited trimer to neighboring trimers is about an order of magnitude greater at 80 K than at 4 K where kT is much smaller than the 30 cm^{-1} splittings between the three lowest energy states. That is, the first step of the process that leads to quenching is escape of excitation from the initially excited trimer to neighboring trimers. The other two steps are migration of the excitation (exciton) to the trapping site(s) and capture of the excitation by the quenching state(s) which, interestingly, is highly nonradiative. The model also explains why the dependence of the quenching is weak at temperatures higher than about 80 K ($kT \sim 55$ cm^{-1}). It was determined that, in the low-temperature limit, intertrimer energy transfer occurs no faster than 50 ps.

The hole spectra identified low energy absorption in the aggregate centered at 684 nm with a large width of 240 cm^{-1} which was assigned to the previously identified red-emitting states that carry nanosecond lifetimes. These states are not the quenching states.[11,12] The nature of the latter, which are highly nonradiative, remains to be determined although it seems likely that they are connected with interactions between Chl *a* molecules of the minor protein complexes with those of the LHC II trimer.[12] To understand the aggregation-induced quenching, experiments should be performed on aggregate samples in which the amounts of the minor complexes are varied. More detailed time-resolved fluorescence experiments are required to determine whether exciton migration is the rate-limiting step in the quenching process.

Acknowledgment. Research at the Ames Laboratory was supported by the Division of Chemical Sciences, Office of Basic Energy Sciences, U.S. Department of Energy (USDOE). Ames Laboratory is operated for USDOE by Iowa State University under Contract W-7405-Eng-82. J.P. gratefully acknowledges support by NaFöG, the German Academic Exchange Service (DAAD), and the International Institute of Theoretical and Applied Physics (IITAP) in Ames. K.-D.I., J.V., and G.R. acknowledge financial support from Deutsche Forschungsgemeinschaft (SFB 312, TP A2, and A6).

References and Notes

(1) Renger, G. In *Topics in Photosynthesis, The Photosystems: Structure, Function and Molecular Biology*; Barber, J., Ed.; Elsevier: Amsterdam, 1992; pp 45−99.

(2) van Grondelle, R.; Dekker: J. P.; Gillbro, T.; Sundstrom, V. *Biochim. Biophys. Acta* **1994**, *1187*, 1.

(3) Horton, P.; Ruban, A. V.; Walters, R. G. *Annu. Rev. Plant Physiol. Plant Mol. Biol.* **1996**, *47*, 655.

(4) Jansson, S. *Biochim. Biophys. Acta* **1994**, *1184*, 1.

(5) Zucchelli, G.; Dainese, P.; Jennings, R. C.; Breton, J.; Garlaschi, F. M.; Bassi, R. *Biochemistry* **1994**, *33*, 8982.

(6) Paulsen, H. *Photochem. Photobiol.* **1995**, *62*, 367.

(7) Green, B. R.; Dunford, D. G. N. *Annu. Rev. Plant Physiol. Plant Mol. Biol.* **1996**, *47*, 685.

(8) Bassi, R.; Sandora, D.; Croce, R. *Physiol. Plant.* **1997**, *100*, 769.

(9) Pieper, J.; Rätsep, M.; Jankowiak, R.; Irrgang, K.-D.; Voigt, J.; Renger, G.; Small, G. J. *J. Phys. Chem. B*, **1999**, *103*, 2412.

(10) Kühlbrandt, W.; Wang, D. N.; Fujiyoshi, Y. *Nature* **1994**, *367*, 614.

(11) Mullineaux, C. W.; Pascal, A. A.; Horton, P.; Holzwarth, A. R. *Biochim. Biophys. Acta* **1993**, *1141*, 23.

(12) Vasiliev, S.; Irrgang, K.-D.; Schrötter, T.; Bergmann, A.; Eichler, H.-J.; Renger, G. *Biochemistry* **1997**, *36*, 7503.

(13) Ruban, A. V.; Horton, P. *Biochim. Biophys. Acta* **1992**, *1102*, 30.

(14) Ruban, A. V.; Dekker: J. P.; Horton, P.; van Grondelle, R. *Photochem. Photobiol.* **1995**, *61*, 216.

(15) Burke, J. J.; Ditto, C. I.; Arntzen, C. *Arch. Biochem. Biophys.* **1978**, *187*, 252.

(16) Irrgang, K.-D.; Boekema, E. J.; Vater, J.; Renger, G. *Eur. J. Biochem.* **1988**, *178*, 207.

(17) Ruban, A. V.; Horton, P.; Robert, B. *Biochemistry* **1995**, *34*, 2333.

(18) Ruban, A. V.; Calcoen, F.; Kwa, S. L. S.; van Grondelle, R.; Horton, P.; Dekker: J. P. *Biochim. Biophys. Acta* **1997**, 1321, 61.

(19) Schödel, R.; Irrgang, K.-D.; Voigt, J.; Renger, G. *Biophys. J.* **1998**, in press.

(20) Porra, R. G.; Thompson, W. A.; Kriedemann, P. E. *Biochim. Biophys. Acta* **1989**, *975*, 384.

(21) Voigt, J.; Renger, Th.; Schödel, R.; Schrötter, Th.; Pieper, J.; Redlin, H. *Phys. Status Solidi B* **1996**, *194*, 333.

(22) Hayes, J. M.; Lyle, P. A.; Small, G. J. *J. Chem. Phys.* **1994**, *91*, 7337.

(23) Savikhin, S.; van Amerongen, H.; Kwa, S. L. S.; van Grondelle, R.; Struve, W. S. *Biophys. J.* **1994**, *66*, 1597.

(24) Lyle, P. A.; Kolaczkowski, S. V.; Small, G. J. *J. Phys. Chem.* **1993**, *97*, 6924 and references cited therein.